Tellus (1979), **31**, 432–446

Observational and theoretical evidence in support of a significant in-situ photochemical source of tropospheric ozone

By JACK FISHMAN, *Department of Atmospheric Science, Colorado State University, Ft. Collins, Colorado 80523, U.S.A.*, SUSAN SOLOMON, *National Centre for Atmospheric Research,*[1] *P.O. Box 3000, Boulder, Colorado 80307, U.S.A.* and *Department of Chemistry, University of California, Berkeley, Berkeley, California 94720, U.S.A.*, and PAUL J. CRUTZEN, *National Centre for Atmospheric Research,*[1] *P.O. Box 3000, Boulder, Colorado 80307, U.S.A.*

(Manuscript received December 20, 1978; in final form May 3, 1979)

ABSTRACT

The latitudinal and seasonal variation of ozone in the troposphere is discussed. Of particular interest is the asymmetrical behavior of this gas with respect to the two hemispheres. These asymmetries, when coupled with a diagnostic photochemical model of the troposphere, lends support to the view that ozone cannot be viewed as an inert tracer of stratospheric origin. We note in our calculations that it is likely that the budgets of carbon monoxide and tropospheric ozone may be quite dependent on each other and discuss these calculations in light of the uncertainty which currently exists about representative global tropospheric background concentrations of the nitrogen oxides. In addition, the seasonal variation of excess $^{14}CO_2$ (a stratospheric tracer) is examined and compared with the seasonal ozone variation during the same period of observations at the same location and altitudes. The distinct maxima for ozone found during the summer in the lower troposphere are not present for the $^{14}CO_2$ data. This finding likewise suggests that photochemical processes taking place in the troposphere are an important source term for tropospheric ozone.

1. Introduction

In recent years, several studies have been devoted to obtaining the global distribution and budgets of trace gases in the troposphere. Noteworthy among these are the works of Seiler (1974, 1976) which presented the global cycle of carbon monoxide through a diligent analysis of its distribution, sources and sinks. Similar studies have been carried out for methane (Ehhalt, 1974) and molecular hydrogen (Schmidt, 1974). In this study we will examine the tropospheric ozone budget in light of its distribution and the photochemical processes which affect it. The importance of obtaining a clear understanding of the tropospheric ozone budget should not be underestimated. The presence of ozone is a prerequisite in the production of hydroxyl radicals in the troposphere (Levy, 1972; 1973) which, in turn, control the atmospheric cycle of many trace gases released to the atmosphere. For instance several hydrocarbon gases would build up to concentrations orders of magnitude larger than present in the atmosphere, if reaction with OH would not take place. Previous analyses of the global cycle of ozone in the troposphere have always assumed that this gas is photochemically inert in this region of the atmosphere (e.g., Pruchniewicz, 1973; Fabian and Pruchniewicz, 1977). However, Fishman and Crutzen (1977) calculated that approximately half the ozone transported into the troposphere from the stratosphere was destroyed by photochemical processes before reaching the ground. Furthermore, there are photochemical cycles capable of providing a significant in-situ source in the troposphere which can not be neglected in the overall budget of this gas. The

---

[1] The National Centre for Atmospheric Research is sponsored by the National Science Foundation.

0040-2826/79/050432-15$02.50/0

study by Fishman and Crutzen (1977) concluded that extrapolation of a one-dimensional model to derive a tropospheric ozone budget would not be realistic because of the seasonal and latitudinal variation observed in the troposphere for this gas. In addition, they showed how a model-derived tropospheric ozone profile could be manipulated by changing several key photochemical rate constants, eddy diffusion coefficients, or the background concentrations of the nitrogen oxides.

Thus, in this study, we have employed a different method of analysis by developing a diagnostic model to quantify the photochemical production and destruction terms of the tropospheric ozone budget. To utilize such a tool on a global scale, it was necessary to obtain a two-dimensional picture of the distribution of background levels of tropospheric ozone. Chatfield and Harrison (1977a) and Wilcox and Belmont (1977) had presented such analyses for the Northern Hemisphere (NH), but a similar task for the Southern Hemisphere (SH) had not been performed. Thus, we conducted an extensive search through *Ozone Data for the World* (a bi-monthly publication of the Canadian Department of Transportation initiated in 1960) to establish a representative tropospheric ozone distribution in the SH.

In the discussion which follows, we will focus on the observed asymmetry of the distribution of tropospheric ozone between the two hemispheres. This asymmetry, as well as the different seasonal behavior of ozone in the free troposphere in the two hemispheres, suggests that the tropospheric budgets of ozone in the two hemispheres are considerably different. In particular, we will present an analysis which implies that the oxidation of carbon monoxide, methane and other hydrocarbons, in the presence of NO and NO_2 (NO_x) represents an in-situ photochemical source of ozone in the Northern Hemisphere which may dominate the source provided via transport from the stratosphere (Fishman and Crutzen, 1978a). Also in support of this premise, we will show that the seasonal behavior of bomb-produced excess $^{14}CO_2$ data differs from that of tropospheric ozone at the same location during the same period of observations. Since this $^{14}CO_2$ must originate in the stratosphere (from nuclear bomb testing), the fact that the seasonal behavior of ozone is different indicates that tropospheric ozone has an important source other than injection from the stratosphere.

2. The ozone data available for this study

Ozone Data for the World (1960–1977) lists data from five stations in the SH which launched ozonesondes during the 1960's and 1970's, along with occasional ship data. Data from one of these stations (Aspendale, 38° S) consist of more than 700 soundings; these data have previously been analyzed by Pittock (1974, 1977). Only 170 total soundings were available from all the other stations: Canton Island (3° S); La Paz (16° S); Christchurch (43° S); and Syowa (69° S). For the calculations which will be presented later in this paper, all soundings were averaged into three month (seasonal) profiles to minimize the effects of any one anomalous profile. We realize that these data are somewhat sparse, but we are not aware of any better set of SH tropospheric data at this time. This situation cannot be improved until a comprehensive sampling program is developed in the SH, but the prospects of this seem dim since many of the previously operating SH stations have either closed down entirely or reduced their sampling programs. The ozone data for the NH are far more extensive. In the remainder of this section, we will review the available data sets of tropospheric ozone and concentrate on seasonal and hemispheric differences.

2.1. *Ozone data at mid-latitudes*

Because the greatest quantity of data for both hemispheres exist in mid-latitudes, we place primary emphasis on the analysis of these data to derive a representative seasonal variation for each hemisphere. In the NH, data exist from several North American stations which were part of the North American Ozonesonde Network established by the Air Force Cambridge Research Laboratory (Hering and Borden, 1967) and from the measurements of Dütsch (1966) and Dütsch et al. (1970) which summarize data obtained at Boulder, Colorado (40° N) and Thalwil, Switzerland (47° N). In the SH, the data presented by Pittock (1974, 1977) from Aspendale, Australia, (38° S) are the most extensive available from that hemisphere. For this reason we have chosen the data from the same latitude in the NH for our hemispheric comparisons. Thus, in Fig. 1, we show the monthly variation of ozone at Boulder (Dütsch et al., 1970) at 40° N, and the combined data from Bedford (42° N) and Wallops Island (38° N)

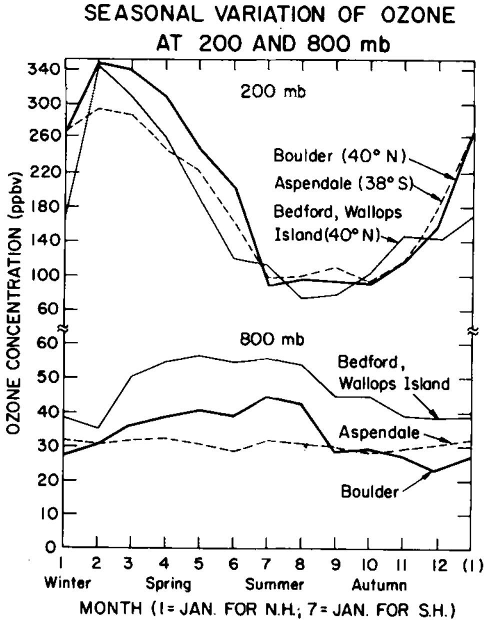

Fig. 1. Monthly variation of ozone for three data sets in the mid-latitudes. The upper curves depict the variation in the upper troposphere (200 mb) whereas the lower set of curves describes the seasonal variations in the lower free troposphere at 800 mb.

(Chatfied and Harrison, 1977), as well as the data from Aspendale (Pittock, 1974; 1977) at 200 mb and 800 mb.

At 200 mb, a distinct annual maximum occurs in the late winter and early spring (months 2, 3, 4) at all stations. In addition, the amplitude of the annual cycle and the absolute concentrations of all three data sets are very similar. The winter maximum of 200 mb correlates well with the annual cycle of total ozone. This feature is the result of downward ozone transport from the stratosphere combined with the fact that the tropopause is lowered during these months implying that the altitude of maximum ozone concentration is closer to the height of the 200 mb level.

Examination of the seasonal variation of the three data sets at 800 mb does not reveal the pronounced similarities among the data sets that are present at 200 mb. In general, we can say that the NH data exhibit a distinct seasonal cycle whereas the SH 800 mb data seasonal variation is quite damped. Furthermore, the average ozone concentration at Aspendale at 800 mb is considerably less than the average values found at the NH mid-latitude stations. Thus, it is clear from the differences seen at 800 mb in the two hemispheres that the processes responsible for the observed concentrations seen in the free troposphere at this level are inherently different. If the assumption is made that meteorological processes represent the primary mechanism providing ozone to the free troposphere, then we should expect to see considerable differences in the mid-latitude downward transport in the two hemispheres. However, examination of meteorological parameters which should be indicative of stratosphere-troposphere exchange in the mid-latitudes do not reveal large hemispheric differences (Fishman and Crutzen, 1978a).

Therefore, it is plausible to postulate that the larger amounts of ozone in the NH are the result of photochemistry, particularly since this difference appears to be most pronounced in the summer. This suggestion will be substantiated in Sectons III and IV.

2.2. *Tropospheric ozone data in the tropics*

The ozone data in the tropics are considerably fewer than those available for mid-latitude regions in both hemispheres. For this study, the NH tropical data consist of 43 soundings from Panama (9° N) whereas the SH tropical data are comprised of 31 ozonesondes from Canton Island (2° S) and 10 from La Paz (16° S). From Fig. 2, it is clear that considerably more ozone is present at every level in the NH tropical troposphere than in the corresponding latitude region in the SH. Integrated throughout the lowest 12 km, the NH column depicted in Fig. 2 is about 6% greater than the corresponding SH profile. Upon a more detailed examination of the ozonesonde data, we can conclude that this hemispheric difference is real and not merely an artifact of differences in the methods of sampling. In light of the discussion of Chatfield and Harrison (1977b), we were concerned about the bias introduced into these average data because of the different types of sondes used in data acquisition. In particular, although all the soundings used to depict the profiles shown in Fig. 2 were taken between 1963 and 1965, Regener chemiluminescent sondes were used entirely for the SH stations, whereas both chemiluminescent and electrochemical sondes were employed at the Panama station. Thus, we examined the individual soundings to determine what effect the use of different instruments had on the tropospheric profiles. Our findings were similar to those of Chatfield and

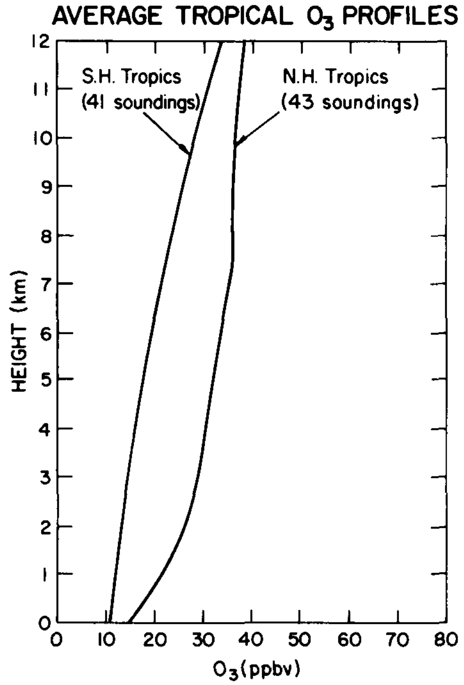

Fig. 2. Average tropospheric ozone profiles for the NH and SH tropics.

Harrison (1977b), but our analysis did not produce the sharp difference between the two types of sondes that were indicated through their examination of the Bedford data. Below 6 km, our analysis indicates that the average ozone concentration measured by the chemiluminescent instrument is 10–20% lower than those measured by the electrochemical sondes. However, between 6 and 12 km, the chemiluminescent data were 5–10% higher than the electrochemical data. Thus, even by using only the data taken with chemiluminescent ozonesondes, a substantial difference on the order of 50% still exists between the average tropospheric ozone content in the NH and SH tropics. Although this finding in the tropics is somewhat surprising, previous measurements of ozone in low-latitude regions likewise have indicated that considerably more ozone is present in the NH tropics than in the SH tropics. For example, Pruchniewicz (1974) has shown that the average tropospheric O_3 concentrations in the region from 0 to 30° N are about 30% higher than those measured between 0 and 30° S. Thus, it is evident from all data sets which we have examined in both tropical and mid-latitude regions, that significantly more tropospheric ozone is present in the NH than in the SH. The implication of this general pattern suggests that either a larger ozone source exists in the NH or that the sink of ozone in the SH is considerably larger. In the next section we will explore the hypothesis that a larger source of ozone in the NH is reasonable in light of photochemical considerations.

3. The budgets of tropospheric ozone and CO and their interdependence

One of the major thrusts of our research has been to examine the role of in-situ photochemical production of ozone in the troposphere to see whether or not this process can account for the observed hemispheric differences. In the unpolluted atmosphere, at least two photochemical oxidation chains have been described which may lead to the production of ozone in the troposphere (Crutzen, 1974; Fishman and Crutzen, 1977). For instance, the oxidation sequence of methane:

R1 $CH_4 + OH \rightarrow CH_3 + H_2O$
R2 $CH_3 + O_2 + M \rightarrow CH_3O_2 + M$
R3 $CH_3O_2 + NO \rightarrow CH_3O + NO_2$
R4 $NO_2 + h\nu \rightarrow NO + O$
R5 $CH_3O + O_2 \rightarrow CH_2O + HO_2$
R6 $HO_2 + NO \rightarrow NO_2 + OH$
R4 $(NO_2 + h\nu \rightarrow NO + O, \lambda < 400\,\text{nm})$
R7 $CH_2O + h\nu \rightarrow H_2 + CO$
R9 $2 \times (O + O_2 + M \rightarrow O_3 + M)$

$$CH_4 + 4O_2 \rightarrow CO + H_2 + H_2O + 2O_2 \text{ (net)}$$

serves as a source for both O_3 and CO in the troposphere. It has recently been suggested that non-methane hydrocarbons produced by natural terpene and isoprene emitters may also produce O_3 and CO (e.g., see Zimmerman et al., 1978). As is well known, other hydrocarbons produced by anthropogenic activity behave similarly, particularly in urban areas. Furthermore, CO in the troposphere, whether its origin is hydrocarbon oxidation or direct injection, likewise is oxidized by OH in the atmosphere to produce ozone:

R10 $CO + OH \rightarrow CO_2 + H$
R11 $H + O_2 + M \rightarrow HO_2 + M$
R6 $HO_2 + NO \rightarrow OH + NO_2$
R4 $NO_2 + h\nu \rightarrow NO + O$
R9 $O + O_2 + M \rightarrow O_3 + M$

$$CO + 2O_2 \rightarrow CO_2 + O_3 \text{ (net)}$$

It should be noted that the primary source of the OH radical involves loss of ozone through the sequence of photolysis

R12 $O_3 + h\nu \rightarrow O_2 + O(^1D) \quad \lambda < 320\ \mathrm{nm}$

followed by the reaction

R13 $O(^1D) + H_2O \rightarrow 2OH$

Subsequently, OH may react with CO, CH_4 or non-methane hydrocarbons in the presence of NO_x to produce ozone, which regenerates OH. Thus, it is clear from the above photochemical sequences that the photochemical cycles which influence CO and O_3 are very independent. Therefore, it is important to examine the global cycles of CO and non-methane hydrocarbons to determine its effect on the global budget and distribution of tropospheric O_3.

In addition, we noted that the production of ozone via these oxidation sequences is critically dependent on the presence of sufficient NO. Since most of the OH in the troposphere reacts with CO, ozone can be destroyed, rather than created, by oxidation of CO if insufficient NO is present by the sequence:

$$\begin{array}{ll} \text{R10} & CO + HO \rightarrow CO_2 + H \\ \text{R11} & H + O_2 + M \rightarrow HO_2 + M \\ \text{R14} & HO_2 + O_3 \rightarrow 2O_2 + OH \\ \hline & CO + O_3 \rightarrow CO_2 + O_2\ (\text{net}) \end{array}$$

Because of the very fast rate constant of the reaction $HO_2 + NO \rightarrow NO_2 + OH$ (Howard and Evenson, 1977), NO volume mixing ratios must be less than 10^{-11} before HO_2 reacts predominantly with O_3 rather than with NO under typical tropospheric conditions. Thus, it is clear that the ozone budget in the troposphere is critically dependent on the tropospheric distribution of the nitrogen oxides (NO_x). The NO_x profiles depicted in Fig. 3 have been prescribed for the model calculations. Curve A is the NO_x distribution assumed for "clean" tropospheric air and is prescribed throughout the SH and southwards of 15° in the NH. Curve B is prescribed at 45° N and northward; intermediate profiles are assumed between 15° N and 45° N. The integrated NO_x tropospheric column density is $2.1 \times 10^{14}\ \mathrm{cm}^{-2}$ for A and $4.6 \times 10^{14}\ \mathrm{cm}^{-2}$ for B. These distributions are consistent with the observations of Noxon (1978) who states that the vertical column density of NO_2 in the troposphere should not exceed $3 \times 10^{14}\ \mathrm{cm}^{-2}$ when local pollution does not influence the measurements. The shape of the profile and the ground level concentrations are likewise consistent with the measurements of Kley et al. (1978) and Drummond (1977).

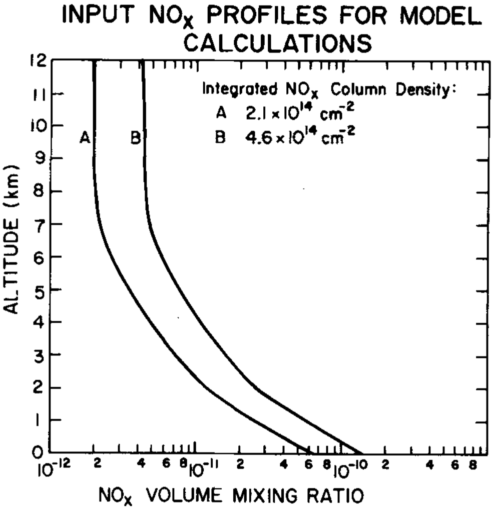

Fig. 3. Prescribed tropospheric NO_x profiles used in the calculation of the ozone, carbon monoxide and methane destruction rates presented in Table 1. Curve A is the NO_x distribution prescribed in the SH and southwards of 15° N in the NH. Curve B is the profile prescribed at 45° N and northwards. Intermediate profiles are assumed between 15° N and 45° N.

The most complete analysis of the global distribution of CO has been conducted by Seiler (1974). From this analysis, we note the uniform decrease in the low altitude CO concentration as one progresses southward from NH mid-latitudes so that there is three times as much CO at 45° N as at 45° S. This factor decreases to 2 in the middle troposphere, whereas equal concentrations are found in the lower stratosphere. Similar trends are observed at other latitudes.

By using the observed distributions of O_3, CO, H_2O and CH_4 and the prescribed profiles of NO_x depicted in Fig. 3, the tropospheric distribution of the hydroxyl radical (OH) can be computed. The globally and diurnally averaged annual OH concentration is presently estimated to be between 3 and $9 \times 10^5\ \mathrm{cm}^{-3}$, based on either the consideration of the CH_3CCl_3 budget (Singh, 1977; Chang and Penner, 1978; Neely and Plonka, 1978) or, independently, on the photochemical model calculations of Crutzen and Fishman (1977) and Derwent and Curtis (1977). We shall use the model-derived

Table 1. *Calculated photochemical destruction rates of various trace gases in the troposphere*

	NH	SH	Global
Photochemical destruction of O_3	20.0	11.0	15.5
From $O(^1D) + H_2O$ (R13)	10.4 (52%)	5.0 (45%)	7.7 (50%)
$O_3 + HO_2$ (R14)	8.5 (42%)	5.2 (42%)	6.8 (44%)
$O_3 + OH$ (R15)	1.1 (6%)	0.8 (8%)	1.0 (6%)
Photochemical oxidation of CO	28.6	19.3	23.9
Photochemical oxidation of CH_4	5.2	6.0	5.6
Injection of O_3 from the stratosphere (Fabian and Pruchniewicz, 1977)	6.8	4.4	5.6

All numbers are in units of 10^{10} molecules cm^{-2} s^{-1}. The percentages in parentheses represent each reaction's contribution to the total amount of gas phase photochemical destruction of ozone as computed by our model.

calculations described in Fishman and Crutzen (1978b) for the analyses given below. A description of the model, and its sensitivity to specific assumptions, is given in Crutzen and Fishman (1977) and in more detail in Fishman and Crutzen (1978b). In the following calculations, the diurnally averaged annual OH distribution for the two hemispheres is approximately 5×10^5 cm^{-3}. Through the manipulation of several key parameters (e.g., the parameterization of heterogeneous removal of water soluble species) within the model, it can be shown that a large range of OH can realistically be calculated (Fishman and Crutzen, 1978b). This uncertainty should be kept in mind during the following discussion, but we feel that the OH distribution used in the presentation of the numbers in Table 1 (which yields a diurnally and seasonally averaged value of 5×10^5 cm^{-3}) is a reasonable choice.

Several important considerations evolve from the numbers presented in Table 1:

(1) From our photochemical model and the distribution of ozone in the troposphere, we calculate a globally averaged photochemical column destruction rate of 15.5×10^{10} mol cm^{-2} s^{-1} due to reactions which yields a lifetime of between one and two months. This lifetime is consistent with lifetimes computed in previous studies which assumed that ozone was photochemically inert in the troposphere (e.g., Fabian and Pruchniewicz, 1977). The most important photochemical destruction reactions for ozone in the troposphere (see Fishman and Crutzen, 1977) are:

R12 $O_3 + h\nu \rightarrow O(^1D) + O_2, \lambda \leq 310\ \text{nm}$

R13 $O(^1D) + H_2O \rightarrow 2OH, k_{13} = 2.3 \times 10^{-10}\ \text{cm}^3\ \text{mol}^{-1}\ \text{s}^{-1}$

R14 $HO_2 + O_3 \rightarrow OH + 2O_2, k_{14} = 1.4 \times 10^{-14}\ e^{-580/T}\ \text{cm}^3\ \text{cm}^3\ \text{mol}^{-1}\ \text{s}^{-1}$

R15 $OH + O_3 \rightarrow HO_2 + O_2, k_{15} = 1.5 \times 10^{-12}\ e^{-1000/T}\ \text{cm}^3\ \text{mol}^{-1}\ \text{s}^{-1}$

From the data in table 1, R13 and R14 contribute nearly equally to ozone destruction. However, R15 destroys about five times less ozone than either R13 or R14. It should be noted that the more recent measurements of k_{14} (e.g., Howard and Zahniser, 1978) are two to six times larger in the troposphere than the values recommended by Hampson and Garvin (1978). Because we have used the new value of k_{14} (from Howard and Zahniser, 1978) this reaction competes with the sequence R12 and R13 to become the primary photochemical loss mechanism of ozone in the troposphere. Using the older values of k_{14}, the reaction of metastable atomic oxygen with water vapor was clearly the major mechanism by which ozone was destroyed photochemically in the troposphere.

(2) If each CO molecule oxidized by OH would yield one ozone molecule by the reaction sequence R10 + R11 + R6 + R4 + R9, the magnitude of the in-situ photochemical source of ozone would be several times larger than the amount of ozone estimated to be transported from the stratosphere: 5.6×10^{10} mol cm^{-2} s^{-1} (Fabian and Pruchniewicz, 1977). Noting that the oxidation of each methane molecule to CO is capable of producing at least two ozone molecules in the presence of sufficient NO, then CO and CH_4 oxidation is potentially capable of providing a source of 39.0×10^{10}

mol cm^{-2} s^{-1} in the NH and 31.3 × 10^{10} mol cm^{-2} s^{-1} in the SH. Thus, if only one-fourth of this resulted in ozone formation, this source would still be comparable to the amount of ozone estimated to come from the stratosphere. In addition we note that more ozone can be produced from the oxidation of methane if the formaldehyde, which is produced by R5, photolyzes to two radicals:

R8 $CH_2O = h\nu \rightarrow CHO + H$

Each of these radicals can, in turn, produce an ozone molecule if sufficient NO is present. Thus, each methane molecule can result in the production of four ozone molecules if this reaction pathway is followed.

R3 $CH_3O_2 + NO \rightarrow CH_3O + NO_2$
R4 $NO_2 + h\nu \rightarrow NO + O\ (\lambda < 400\ \text{nm})$
R5 $CH_3O + O_2 \rightarrow CH_2O + HO_2$
R6 $HO_2 + NO \rightarrow NO_2 + OH$
R7 $CH_2O + h\nu \rightarrow CO + H_2$
R8 $CH_2O + h\nu \rightarrow CHO + H$
R9 $O + O_2 + M \rightarrow O_3 + M$

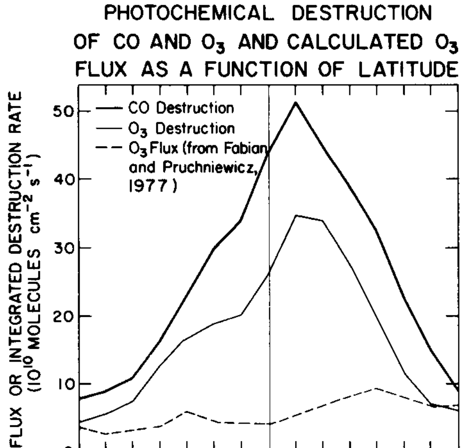

Fig. 4. Model-derived, annual mean, photochemical destruction rates for ozone and carbon monoxide as a function of latitude. Also shown for comparison are the calculated ozone destruction rates at the earth's surface, likewise presented as a function of latitude (from Fabian and Pruchniewicz, 1977).

R10 $CO + OH \rightarrow CO_2 + H$
R11 $H + O_2 + M \rightarrow HO_2 + M$
R12 $O_3 + h\nu \rightarrow O_2 + O(^1D)\ \lambda < 320\ \text{nm}$
R13 $H_2O + O(^1D) \rightarrow 2OH$
R14 $HO_2 + O_2 \rightarrow OH + 2O_2$
R15 $OH + O_3 \rightarrow HO_2 + O_2$
R16 $HO_2 + HO_2 \rightarrow H_2O_2 + O_2$
R17 $HO_2 + OH \rightarrow H_2O + O_2$
R18 $HO_2 + CH_3O_2 \rightarrow CH_3O_2H + O_2$
R19 $H_2O_2 + h\nu \rightarrow 2\,OH$

(3) The ratio of CO oxidation to CH_4 oxidation is 5.5 in the NH, and 3.2 in the SH. This ratio is independent of the amount of OH present in the troposphere and dictates that methane oxidation cannot be the primary source of CO in either hemisphere.

In Fig. 4 we show the computed tropospheric photochemical destruction rates of CO and O_3 as a function of latitude. These destruction rates are compared to the calculated O_3 injection rate from the stratosphere (from Fabian and Pruchniewicz, 1977).

From the photochemical calculations discussed in this section, it is clear that we feel that the photochemistry of tropospheric ozone plays an essential role in the development of a budget for this gas. So far, we have simplified the discussion by examining the likely relationship between the amount of CO photochemically oxidized and the amount of ozone produced photochemically. However, the precise quantification of the photochemical production and destruction terms in the budgets of these gases is critically dependent upon the assumed distribution of NO_x in the troposphere. Because representative global background concentrations of these species are not presently available (Crutzen, 1979) it is difficult to assign numbers without relatively large error bars to the calculated photochemical production and destruction terms in the ozone budget. In the next section, we will examine these photochemical calculations under different assumptions for the background concentrations of the nitrogen oxides. Nevertheless, we can conclude from our calculations that unless our present knowledge of atmospheric chemistry is severely incorrect, the individual photochemical production and destruction terms in the tropospheric ozone budget are comparable to (and most likely larger than) either the amount of O_3 injected from the stratosphere or the subsequent destruction rate at the ground.

4. Sensitivity of the calculations to assumed NO_x concentrations

Previous studies of tropospheric chemistry have shown that the net production of ozone in the troposphere is critically dependent on the background concentration of NO_x (e.g., see Fishman and Crutzen, 1977; Chameides, 1978). In general, it can be stated that the formation of ozone takes place when reaction with a peroxy radical, RO_2, converts NO to NO_2. The subsequent photolysis of NO_2 in the troposphere results in the production of ozone. This process appears to be quite efficient since the reaction of NO and HO_2 has been measured to proceed very rapidly (Howard and Evenson, 1977) and it is likely that other peroxy radical reactions with NO proceed just as efficiently (Cox, personal communication). In addition, the above ozone producing cycle is catalytic which means that NO is still available for further ozone production once the cycle is completed. Thus, once the RO_2 radical is formed, ozone will be produced unless one of the following occurs:

(1) The RO_2 radical reacts with a species other than NO; or
(2) NO_2 reacts with something in the atmosphere before it can photodissociate.

The latter possibility is rather unlikely. Comparing a typical NO_2 photolysis rate 5×10^{-3} s^{-1} (Stedman et al., 1975) with other possible reaction pathways for NO_2 in the unpolluted troposphere, it is clear that much more than 95% of the NO_2 will photolyze rather than react with something else. For example, the production of nitric acid,

$$NO_2 + OH\,(+M) \rightarrow HNO_3\,(+M)$$

is the second most likely pathway (after photolysis) for NO_2 in the troposphere. With an equivalent tropospheric two body rate constant of 8×10^{-12} $cm^3\ mol^{-1}\ s^{-1}$ (Hampson and Garvin, 1978) even

Table 2. *Competition of reactions involving the HO_2 radical for representative tropospheric boundary layer daytime conditions and various concentrations of NO*

Reaction	Reactant concentration (mol cm^{-3})	Rate of reaction (s^{-1})	Fraction
Case 1: NO volume mixing ratio = 5×10^{-12}			
$HO_2 + NO \rightarrow OH + NO_2$	$NO = 1.0 \times 10^8$	8.0×10^{-4}	0.16
$HO_2 + O_3 \rightarrow OH + 2O_2$	$O_2 = 8.0 \times 10^{11}$	1.4×10^{-3}	0.27
$HO_2 + HO_2 \rightarrow H_2O_2 + O_2$	$HO_2 = 6.0 \times 10^8$	1.9×10^{-3}	0.37
$HO_2 + OH \rightarrow H_2O + O_2$	$OH = 2.0 \times 10^6$	1.0×10^{-3}	0.02
$HO_2 + CH_3O_2 \rightarrow CH_3O_2H + O_2$	$CH_2O_2 = 3.0 \times 10^8$	9.3×10^{-4}	0.18
Case 2: NO volume mixing ratio = 10×10^{-12}			
$HO_2 + NO \rightarrow OH + NO_2$	$NO = 2.0 \times 10^8$	1.6×10^{-3}	0.27
$HO_2 + O_3 \rightarrow OH + 2O_2$	$O_3 = 8.0 \times 10^{11}$	1.4×10^{-3}	0.24
$HO_2 + HO_2 \rightarrow H_2O_2 + O_2$	$HO_2 = 6.3 \times 10^8$	1.9×10^{-3}	0.32
$HO_2 + OH \rightarrow H_2O + O_2$	$OH = 2.4 \times 10^6$	1.2×10^{-4}	0.02
$HO_2 + CH_3O_2 \rightarrow CH_3O_2H + O_2$	$CH_2O_2 = 3.3 \times 10^8$	9.9×10^{-4}	0.16
Case 3: NO volume mixing ratio = 20×10^{-12}			
$HO_2 + NO \rightarrow OH + NO_2$	$NO = 4.0 \times 10^8$	3.2×10^{-3}	0.42
$HO_2 + O_3 \rightarrow OH + 2O_2$	$O_3 = 8.0 \times 10^{11}$	1.4×10^{-3}	0.18
$HO_2 + HO_2 \rightarrow H_2O_2 + O_2$	$HO_2 = 6.6 \times 10^8$	1.9×10^{-3}	0.25
$HO_2 + OH \rightarrow H_2O + O_2$	$OH = 3.2 \times 10^6$	1.6×10^{-4}	0.02
$HO_2 + CH_3O_2 \rightarrow CH_3O_2H + O_2$	$CH_3O_2 = 3.3 \times 10^8$	1.0×10^{-3}	0.13
Case 4: NO volume mixing ratio = 50×10^{-12}			
$HO_2 + NO \rightarrow OH + NO_2$	$NO = 1.0 \times 10^9$	8.0×10^{-3}	0.62
$HO_2 + O_3 \rightarrow OH + 2O_2$	$O_3 = 8.0 \times 10^{11}$	1.4×10^{-3}	0.11
$HO_2 + HO_2 \rightarrow H_2O_2 + O_2$	$HO_2 = 6.9 \times 10^8$	2.1×10^{-3}	0.16
$HO_2 + OH \rightarrow H_2O + O_2$	$OH = 5.6 \times 10^6$	2.8×10^{-4}	0.02
$HO_2 + CH_3O_2 \rightarrow CH_3O_2H + O_2$	$CH_3O_2 = 3.4 \times 10^8$	1.2×10^{-3}	0.09

with a very high OH concentration of 10^7 cm^{-3}, the rate of removal of NO_2 is less than 2% of the rate of photolysis. Thus, the percentage of ozone produced from each RO_2 radical in the clean troposphere is most critically dependent on the amount of NO which is present in the atmosphere relative to the amount of other species with which RO_2 can react. The remainder of this section will examine this aspect of the calculations.

To assess the impact of the photochemical calculations, we will first examine the various reactions of the RO_2 radical. To simplify the discussion, we will look only at the reactions involving HO_2 and assume that analogies can be made for other peroxy radicals. In our model (Crutzen and Fishman, 1977; Fishman and Crutzen, 1978b) HO_2 can react as follows:

R6 $HO_2 + NO \rightarrow OH + NO_2$;
$k_6 = 8.0 \times 10^{-12}$ cm^3 mol^{-1} s^{-1}
R14 $HO_2 + O_3 \rightarrow OH + 2O_2$;
$k_{14} = 1.8 \times 10^{-15}$ cm^3 mol^{-1} s^{-1}
R16 $HO_2 + HO_2 \rightarrow H_2O_2 + O_2$;
$k_{16} = 3.1 \times 10^{-12}$ cm^3 mol^{-1} s^{-1}
R17 $HO_2 + OH \rightarrow H_2O + O_2$;
$k_{17} = 5.1 \times 10^{-11}$ cm^3 mol^{-1} s^{-1}
R18 $HO_2 + CH_3O_2 \rightarrow CH_3O_2H + O_2$;
$k_{18} = k_{14} = 3.1 \times 10^{-12}$ cm^3 mol^{-1} s^{-1}

The rate constants for each of the above reactions are given for a representative tropospheric temperature of 285 °K and for an altitude of about 2 km.

In Table 2, we summarize the fate of the HO_2 radical under various concentrations of NO. In the first case, when NO volume mixing ratios are 5×10^{-12}, we note that more HO_2 reacts with O_3 than with NO, which enhances the efficiency of the ozone-destroying catalytic cycle relative to that of the ozone-producing sequence of reactions. At an NO concentration of 10×10^{-12} v/v, the HO_2 radical reacts about equally with both NO and O_3. In both these cases, where NO values are very low, it is seen that reaction of HO_2 (or CH_3O_2) with itself (or other peroxy radicals) to form a peroxide dominate the fate of the HO_2 radical. Under such a reaction sequence, the oxidation of CO by OH has no net effect on the tropospheric ozone budget:

R10 $CO + OH \rightarrow CO_2 + H$ (twice),
R11 $H + O_2 + M \rightarrow HO_2 + M$ (twice),
R15 $HO_2 + HO_2 \rightarrow H_2O_2 + O_2$, and
R19 $H_2O_2 + h\nu \rightarrow 2OH$

$$2CO + O_2 \rightarrow 2CO_2 \text{ (net)}$$

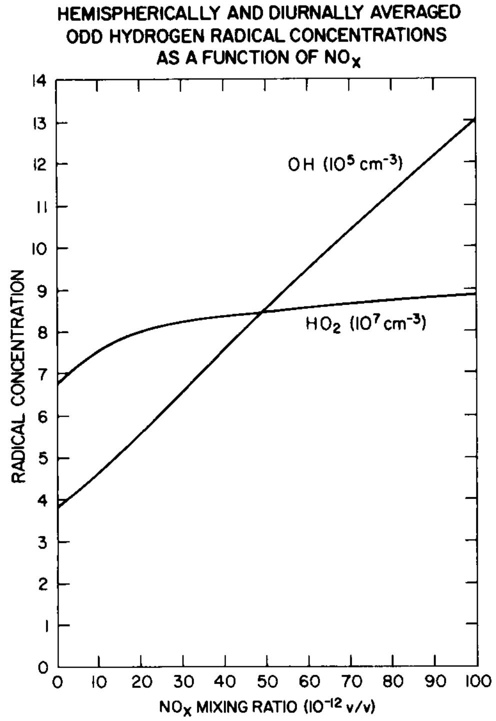

Fig. 5. Model-derived NH average tropospheric OH and HO_2 number densities as a function of prescribed NO_x concentration.

Since H_2O_2 is removed heterogeneously very efficiently in the model calculations at a rate of 2×10^{-5} s^{-1} at ground level, the greater relative production of it when NO concentrations are very low results in an overall loss for the sum of odd hydrogen radicals. Thus, we observe in Fig. 5 that both OH and HO_2 number densities increase as NO_x concentrations increase between volume mixing ratios of 1 and 100×10^{-12}. In other calculations for which we assumed a heterogeneous removal rate on the order of 1×10^6 s^{-1} at ground level (not presented here), we note that HO_2 number densities decrease as NO_x volume mixing ratios approach 50×10^{-12} v/v. The rate at which peroxides are removed heterogeneously from the atmosphere is still open to much speculation and it is clear that the interpretation of many tropospheric calculations are critically dependent on the assumed behavior of species removed heterogeneously (see Crutzen and Fishman, 1977).

Although the sum of the radicals (which is dominated by the amount of HO_2 calculated) only goes up slightly as NO is increased, the OH concentration goes up significantly since its ratio to

Table 3. *Northern hemisphere photochemical production and destruction rates of O_3, CO and CH_4 in the troposphere*

NO_x Concentration (10^{-12} v/v)	1	10	20	25	30	50	75	100
Hemispherically averaged OH (10^5 cm^{-3})	3.78	4.67	5.62	6.10	6.58	8.47	10.8	13.1
Hemispherically averaged HO_2 (10^7 cm^{-3})	6.94	7.67	8.03	8.16	8.26	8.55	8.76	8.86
Photochemical production of O_3 ($P[O_3]$)	0.9	8.8	17.5	21.8	26.3	44.0	66.5	88.8
Photochemical destruction of O_3 ($D[O_3]$)	18.8	19.9	20.5	20.8	21.0	21.7	22.4	23.0
$P[O_3]-D[O_3]$	−18.0	−11.1	−3.1	+1.0	+5.2	+22.3	+44.0	+65.8
Photochemical oxidation of CO (D[CO])	25.2	30.1	35.9	38.8	41.6	53.3	67.8	82.0
Photochemical oxidation of CH_4 ($D[CH_4]$)	4.6	5.5	6.4	6.9	7.4	9.4	11.8	14.2
Potential photochemical production of O_3:								
$Pot[O_3] = D[CO] + 2 \times D[CH_4]$	34.2	41.1	48.7	52.6	56.4	72.1	91.4	110.4
$\frac{P[O_3]}{Pot[O_3]}$	0.03	0.21	0.36	0.41	0.47	0.61	0.73	0.80
Photochemical loss of O_3 broken down by reaction:								
$H_2O + O(^1D)$	10.4	10.4	10.4	10.4	10.4	10.4	10.4	10.4
$HO_2 + O_3$	7.7	8.5	8.9	9.0	9.2	9.5	9.7	9.9
$OH + O_3$	0.9	1.1	1.3	1.4	1.5	1.9	2.4	2.4
Total	18.8	19.9	20.5	20.8	21.0	21.7	22.4	23.0

Note: Units on the photochemical production and destruction are 10^{10} molecules cm^{-2} s^{-1}.

HO_2 is largely controlled by the amount of NO present. We should point out that the OH concentration will eventually reach a maximum as NO_x concentrations approach values near 0.5×10^{-9} v/v (similar to the findings of Hameed et al., 1979). However, it will be shown later in this section that consideration of globally averaged tropospheric NO_x mixing ratios greater than 0.1×10^{-9} v/v is not relevant in light of the tropospheric budget of ozone.

Further examination of Table 2 shows that as NO concentrations increase to 20×10^{-12} v/v and larger, the ozone production pathways of CO and CH_4 oxidation become dominant. Thus, there are two coupled factors which result in increased photochemical production of tropospheric ozone as NO_x concentrations become larger:

(1) Larger NO_x concentrations (for the ranges being considered in these calculations) increase the average concentration of OH which means that more CO and CH_4 oxidation takes place for fixed amounts of CO and CH_4; and

(2) The efficiency of the percentage of ozone produced from the oxidation of CO and CH_4 increases as NO_x concentrations increase.

In Table 3 and Fig. 6, we present the photochemical production and destruction rate of O_3, CO and CH_4 in the NH troposphere. For these calculations, we prescribed the NO_x concentrations listed at the top of each column in Table 2 at every latitude and altitude in the NH. The reader should

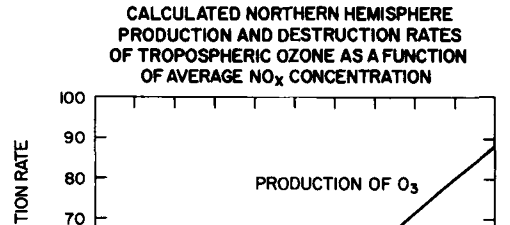

Fig. 6. Model-derived, annual mean, photochemical production and destruction rates of tropospheric ozone in the NH as a function of the prescribed NO_x concentrations.

note that the hemispheric calculations depicted in but that the representative calculations described by Table 2 are presented as a function of NO. We assume that NO and NO_2 are in photochemical equilibrium with each other (see Fishman and Crutzen, 1977) for these calculations and that the Table 3 and Fig. 6 are shown as a function of NO_x, NO to NO_x ratios range typically between 0.2 and 0.5 in the troposphere depending on the amount of O_3 present.

The calculations summarized by this table and figure show very clearly that photochemical production of ozone in the troposphere is nearly a linear function of the amount of NO_x assumed to be present in the model. (This relationship holds for NO_x values up to approximately 0.25×10^{-9} v/v; ozone production as a function of NO_x increases more slowly after that point and gross O_3 production reaches a maximum when NO_x concentrations approach 0.7×10^{-9} v/v.) On the other hand, the amount of ozone destroyed photochemically in the NH troposphere remains fairly constant at a value near 20×10^{10} mol cm^{-2} s^{-1}, regardless of how much NO_x is present. When we look at the individual reactions in Table 3 which are responsible for ozone loss in the troposphere, this finding is not surprising. The dominant photochemical loss mechanisms for ozone are photolysis of O_3 to form $O(^1D)$, which in turn reacts with H_2O to form OH, and reaction of O_3 with HO_2. The amount of ozone destroyed by the first reaction does not change as a function of NO_x since it is primarily dependent on the amount of O_3 and H_2O prescribed in the calculations. Both these quantities remain fixed for the calculations described herein. In addition, the amount of HO_2 calculated by the model increases only slightly as NO_x concentration is increased. Since these two reactions account for approximately 90% of the photochemical destruction of tropospheric ozone, it is readily explainable why total photochemical loss of O_3 remains nearly constant.

Because the amount of ozone lost photochemically in the NH troposphere is relatively constant at a value near 20×10^{10} mol cm^{-2} s^{-1}, some inferences can be made about the other terms which comprise the tropospheric ozone budget: photochemical, net, in-situ production; destruction at the ground; and injection from the stratosphere. To do this, the assumption must be made that the absolute value of the hemispheric photochemical destruction of ozone in the troposphere is not seriously in error. We feel that this is the case since our computed photolysis rate of O_3 to form $O(^1D)$ is in relatively good agreement with those measured directly by Dickerson et al. (1979) and Hanser and Sellers (1979). The magnitude of the photochemical destruction of tropospheric ozone is several times larger than previous estimates of either stratospheric injection or destruction by contact with the ground (Fabian and Junge, 1970; Fabian and Pruchniewicz, 1977; Danielsen and Mohnen, 1977). The uncertainty involved in the latter calculations is at least a factor of two, so that the difference in these terms may approach about 10×10^{10} mol cm^{-2} s^{-1}. Depending on which term is larger than the other, the tropospheric photochemical production rate of ozone must range between 10 and 30×10^{10} mol cm^{-2} s^{-1}. If stratospheric injection is less than ground destruction, the amount of ozone photochemically produced in the troposphere must be the sum of the photochemical destruction term (29×10^{10} mol cm^{-2} s^{-1}) plus the difference between the amount destroyed at the ground and the amount coming from the stratosphere. Examination of Fig. 6 shows that a tropospheric production rate reflecting this range of values corresponds to average tropospheric NO_x mixing ratios ranging between 12 and 35×10^{-12} v/v.

Lastly, in this section, we would like to point out that we have simplified the discussion of these calculations by prescribing uniform amounts of NO_x at every latitude and altitude in the NH. In reality, however, NO_x most likely exhibits a non-homogeneous distribution. Thus, it follows that there may be specific regions and altitudes where photochemical production is the dominant source of tropospheric ozone and that there likewise exist locations where it can be shown that injections from the stratosphere control the observed concentrations of tropospheric ozone. Examples of the latter phenomenon occur on relatively short time scales and can be fairly easily observed by aircraft measurements (e.g., Danielsen 1968; Danielsen and Mohnen, 1977). On the other hand, photochemical production of ozone in the "unpolluted" troposphere takes place on substantially longer time scales, and is not readily detectable. In the next section, however, we do present some data which may be indicative of significant in-situ photochemical production of ozone in the troposphere.

5. Further evidence favoring photochemical production of ozone

The value of the use of tracers in the study of the dispersion of gases in the atmosphere has long been recognized (see e.g., Junge, 1963). Excess $^{14}CO_2$ is a by-product of nuclear bomb explosions, which often reach the stratosphere, and is one of the few radioactive tracers which remain gaseous. Thus, it is an excellent tracer for atmospheric motions (see e.g., Johnston et al., 1976). In this section we will examine the seasonal trends of excess $^{14}CO_2$ in the troposphere over New Mexico (Telegadas, 1971) compared to those of ozone. We note that the vertical profiles of $^{14}CO_2$ and ozone are quite similar in the upper troposphere and lower stratosphere at mid-latitudes. Thus, if ozone is produced uniquely in the stratosphere and is inert in the troposphere as the excess $^{14}CO_2$ is, then similarities should be present in their seasonal trends.

The amount of excess $^{14}CO_2$ data available for seasonal analysis is extremely limited. The summary of Telegadas (1971) shows that these were four locations in the world at which $^{14}CO_2$ vertical distribution measurements were conducted with any regularity. These were located in the NH at 9° N, 35° N and 71° N whereas nearly all the SH vertical profiles were taken at 45°S. The best record of $^{14}CO_2$ data is at 35° N (New Mexico) for which measurements were made between 1955 and 1969. Fortunately ozonesonde data are likewise available from New Mexico between September, 1963 and January, 1966.

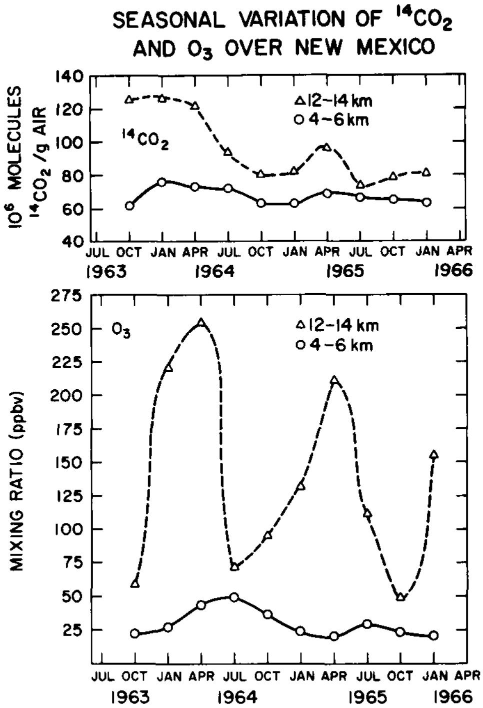

Fig. 7. Seasonal variation of excess $^{14}CO_2$ and tropospheric ozone over New Mexico. The upper set of curves shows the seasonal variation of $^{14}CO_2$ at altitudes representative of the lower stratosphere and middle troposphere. The lower set of curves depicts the seasonal variation of ozone at similar altitudes.

Examination of Fig. 7 shows that the seasonal maxima of $^{14}CO_2$ at altitudes representative of both the lower stratosphere and middle troposphere are in phase. In 1964, both maxima occur in winter whereas in 1965, both occur during the spring. However, the maxima for ozone in the 12–14 km layer occur in spring for both years whereas the maximum takes place in summer at an altitude representative of the middle troposphere. Since the data shown in Fig. 5 are from the same location during the same period of time, we can assume that the meteorological processes affecting both data sets are identical. Thus, it is difficult to explain the delay in the mid-tropospheric ozone maximum solely by mixing processes since a similar seasonal delay is not seen in the $^{14}CO_2$ measurements. Therefore, we can attribute the summer ozone maximum seen in both years at 5 km to something other than a physical mechanism and suggest that photochemical production of tropospheric ozone is responsible for this feature.

It should be noted that excess $^{14}CO_2$ may not be directly comparable to ozone as a tracer for stratospheric injection. This is due to differences in the sinks and resulting residence times of the two gases. It is particularly important that comparison not be made using surface concentrations, which may be quite strongly affected by local sinks, more so than measurements in the free troposphere. However, box model studies of the transfer of $^{14}CO_2$ between its various reservoirs (Nydal, 1968; Young and Fairhall, 1968) have concluded that the observed seasonal variation in tropospheric excess $^{14}CO_2$ is due to the seasonal stratospheric injection. Furthermore, these studies also indicate that the majority of the excess $^{14}CO_2$ is taken up by the oceans.

Young and Fairhall (1968) have calculated the flux of excess $^{14}CO_2$ into the oceans using a model including eddy diffusion and meridional motion as well as laboratory measurements of $^{14}CO_2$ uptake. They calculate a global flux of $^{14}CO_2$ into the oceans of 103×10^{26} atoms over a six-month period. This corresponds to a deposition velocity of about 0.002 cm s^{-1}, somewhat less than that of ozone. Since the deposition velocity of $^{14}CO_2$ is unlikely to be greater than that of ozone if the analysis given above is correct, then the tropospheric residence time of $^{14}CO_2$ should be larger than that of ozone. Thus it is difficult to see how the phase lag observed for ozone could exceed that of $^{14}CO_2$ if ozone is photochemically inert in the troposphere.

6. Summary and conclusions

The fundamental objectives of this paper were to show (a) that important photochemical reactions affecting ozone take place in the troposphere; (b) to present a reasonable tropospheric ozone budget; (c) that it is possible to interpret existing data in a way which suggests that this in-situ photochemical production can be inferred from observations. In particular, important seasonal and latitudinal differences exist in the distribution of tropospheric ozone for the two hemispheres. Some of the primary interhemispheric differences are:

- There is more tropospheric ozone in the NH than in the SH;
- At NH midlatitudes, a free tropospheric seasonal maximum is consistently seen during the summer at low altitudes whereas no obvious seasonal variation is observed in the SH.

Furthermore, because the surface destruction in the NH is three times larger than the corresponding SH destruction rate (Pruchniewicz, 1974; Fishman and Crutzen, 1978a), a corresponding difference must exist in the source terms of tropospheric O_3. The difference in the source terms can not be easily attributed to meteorological influences (Fishman and Crutzen, 1978a). Some additional information which suggests that ozone cannot be treated as an inert substance in the troposphere is provided by comparison of its seasonal behavior with that of $^{14}CO_2$. Whereas the seasonal trends in $^{14}CO_2$ are in phase at 5 and 13 km, a delay of one season is characteristic for NH mid-latitude ozone data. In addition, we have shown that the amount of CO oxidized and subsequent photochemical production of O_3 may exceed the amount of ozone estimated to be transported through the tropopause at nearly every latitude. Since CO oxidation is so much greater in the NH, and since this process is enhanced during the summer, we conclude that the observations support the hypothesis that photochemical production may be a significant source of ozone in the NH troposphere.

Lastly, we must point out what superficial analysis of existing ozone data will not support the hypothesis that photochemical production of ozone in the troposphere is an important source term. Even if nearly all the CO oxidized on a global scale results in the formation of ozone, a computed globally averaged oxidation rate 4×10^{11} mol cm^{-2} s^{-1} translates to an ozone production rate on the order of one part per billion per day at a representative point in the free troposphere. Unlike stratospheric intrusions which are detected readily from aircraft data and are associated with low water vapor concentrations, which likewise are observed from such measurements, the aforementioned photochemical process is widespread and therefore would be very difficult to identify. Alternatively, a long-term monitoring program of CO, NO and O_3 in the background troposphere may provide a more useful data base from which a better understanding of the role of photochemical generation of ozone can be obtained. Hopefully, the establishment of such baseline stations will become a reality. Analysis of the data from these stations may provide the information needed to prove or disprove our contention that the in-situ photochemical production of tropospheric ozone is indeed a significant quantity.

7. Acknowledgements

This research has been supported in part by Grant 804921 from the environmental Protection Agency and Contract NAS1-15129 from the National Aeronautics and Space Administration to Colorado State University. One of us (SS) has been supported under the University Corporation for Atmospheric Research Fellowship Program.

REFERENCES

Chameides, W. L. (1978). The photochemical role of tropospheric nitrogen oxides. *Geophys. Res. Lett. 5*, 17–20.

Chatfield, R. B. and Harrison, H. (1977a). Tropospheric ozone 2. Variations along a meridional band. *J. geophys. Res. 82*, 5969–5976.

Chatfield, R. B. and H. Harrison (1977b). Tropospheric ozone 1. Evidence for higher background concentrations. *J. geophys. Res. 82*, 5965–5968.

Chang, J. S. and Penner, J. E. (1978). Analysis of global budgets of halocarbons. *Atmos. Env.* (in press).

Crutzen, P. J. (1974). Photochemical reactions initiated by and influencing ozone in unpolluted tropospheric air, *Tellus 26*, 47–57.

Crutzen, P. J. (1979). The role of NO and NO_2 in the chemistry of the troposphere and stratosphere. *Annual Review of Earth and Planetary Sciences* (in press).

Crutzen, P. J. and Fishman, J. (1977). Average concentrations of OH in the troposphere and the budgets of CH_4, CO, H_2 and CH_3CCl_3. *Geophys. Res. Lett. 4*, 321–324.

Danielsen, E. F. (1968). Stratospheric-tropospheric exchange of radioactivity, ozone, and potential vorticity. *J. Atmos. Sci. 25*, 502–518.

Danielsen, E. F. and Mohnen, V. A. (1977). Project DUSTORM report: Ozone transport, in-situ measurements, and meteorological analyses of tropopause folding. *J. geophys. Res. 82*, 5867–5878.

Derwent, R. G. and Curtis, A. R. (1977). Two dimensonal model studies of some trace gases and free radicals in the troposphere. Report AERE-R 8853, U.K. Atomic Energy Authority AERE Harwell, Oxfordshire, England.

Dickerson, R. R., Stedman, D. H., Chameides, W. L., Crutzen, P. J. and Fishman, J. (1979). Actinometric measurement and theoretical calculation of the rate of photolysis of ozone to $O(^1D)$. (Submitted to *Geophys. Res. Lett.*)

Drummond, J. W. (1977). Measurement of NO using a chemiluminescent detector, Ph.D. Thesis, Dept. of Physics, University of Wyoming, Laramie.

Dütsch, H. U. (1966). Five years of regular ozone soundings over Boulder. NCAR Tech. Note NCAR-TN-10. National Center for Atmospheric Research, Boulder, Colorado.

Dütsch, H. U., Züllig, W. and Ling, Ch. (1970). Regular ozone observations at Thalwil, Switzerland and at Boulder, Colorado. Report LAPETH-1, Laboratorium für atmosphären physiks ETH, Zurich, Switzerland.

Ehhalt, D. H. (1974). The atmospheric cycle of methane. *Tellus 26*, 58–70.

Fabian, P. and Pruchniewicz, P. G. (1977). Meridional distribution of ozone in the troposphere and its seasonal variation. *J. geophys, Res. 82*, 2063–2073.

Fishman, J. and Crutzen, P. J. (1977). A numerical study of tropospheric photochemistry using a one-dimensional model. *J. geophys. Res. 82*, 5897–5906.

Fishman, J. and Crutzen, P. J. (1978a). The origin of ozone in the troposphere. *Nature, Lond. 274*, 855–858.

Fishman, J. and Crutzen, P. J. (1978b). The distribution of the hydroxyl radical in the troposphere. Atmos. Sci. Paper 284 (Dept. of Atmos. Sci., Colorado State University, Ft. Collins, CO).

Hameed, S., Pinto, J. P. and Stewart, R. W. (1979). Sensitivity of the prediction CO—OH—CH_4 perturbation to tropospheric NO_x, *J. geophys. Res. 84*, 763–768.

Hampson, R. F., Jr. and Garvin, D. (1978). Reaction rate and photochemical data for atmospheric chemistry—1977. NBS Special Publication 513, Dept. of Commerce, Washington, D.C., 111 pp.

Hanser, F. A. and Sellers, B. (1979). Variations of $O(^1D)$ photoproduction rate for the 1977 GAMETAG flights. (Submitted to *J. geophys. Res.*)

Hering, W. S. and Borden, T. R. (1967). Ozonesonde observations over North America, Vols. 1–4, AFCRL-64-30 (I–IV).

Howard, C. J. and Evenson, K. M. (1977). Kinetics of the reaction of HO_2 with NO. *Geophys. Res. Lett. 4*, 437–440.

Howard, C. J. and Zahniser, M. S. (1978). Unpublished data. Presented at WMO Symposium on the Geophysical Aspects of the Consequences of Changes in the Composition of the Stratosphere, Toronto, June 26–30.

Johnston, H. S., Kattenhorn, D. and Whitten, G. Z. (1976). Use of excess carbon 14 data to calibrate models of stratospheric ozone depletion by supersonic transports. *J. geophys. Res. 81*, 368–380.

Junge, C. E. (1963). Studies of global exchange processes in the atmosphere by natural and artificial tracers. *J. geophys. Res. 68*, 3849–3856.

Kley, D., McFarland, M., Drummond, J. W., Schmeltekopf, A. L. (1978). Altitude profile and surface mesurements of tropospheric NO and NO_2. *J. geophys. Res.* (to be submitted).

Levy, H. (1972). Photochemistry of the lower troposphere. *Planet Space Sci. 20*, 919–935.

Levy, H. (1973). Photochemistry of minor constituents in the troposphere. *Planet. Space Sci. 21*, 575–591.

Neely, W. B. and Plonka, J. H. (1978). Estimation of time averaged hydroxyl radical concentration in the troposphere. *Environ. Sci. Technol. 12*, 317–320.

Noxon, J. F. (1978). Tropospheric NO_2. *J. geophys. Res. 83*, 3051–3057.

Nydal, R. (1968). Further investigation on the transfer of radiocarbon in nature, *J. geophys. Res. 73*, 3617–3635.

Ozone Data for the World (1961–1978). Canadian Department of Transportation, Toronto.

Pittock, A. B. (1974). Ozone climatology, trends, and the monitoring problem. Proceedings of the Int. Conf. on

Structure, Composition, and General Circulation of the Upper and Lower Atmospheres and Possible Anthropogenic Perturbations, Melbourne, Australia, 455–461.

Pittock, A. B. (1977). Climatology of the vertical distribution of ozone over Aspendale (38° S 145° E). *Q. Jl R. met. Soc. 103*, 575–585.

Pruchniewicz, P. G. (1973); The average tropospheric ozone content and its variation with season and latitude as a result of the global ozone circulation. *Pure Appl. Geophys. 106–108*, 1058–1073.

Pruchniewicz, P. G. (1974). A study of the tropospheric ozone budget based on interchemispheric mass exchange. Proceedings of the Int. Conf. on Structure, Composition, and General Circulation of the Upper and Lower Atmospheres and Possible Anthropogenic Perturbations, Melbourne, Australia, 429–438.

Schmidt, U. (1974). Molecular hydrogen in the atmosphere. *Tellus 26*, 11–20.

Seiler, W. (1974). The cycle of atmospheric CO. *Tellus 26*, 116–135.

Seiler, W. (1976). The cycle of carbon monoxide in the atmosphere. Proc. ICESA Inst. of Electr. and Electronic Engineers, New York.

Singh, H. B. (1977). Atmospheric halocarbons: evidence in favour of reduced averaged hydroxyl radical concentration in the troposphere. *Geophys. Res. Lett. 4*, 101–104.

Stedman, D. H., Chameides, W. L. and Jackson, J. O. (1975). Comparison of experimental and computed values for j(NO_2), *Geophys. Res. Ltrs. 2*, 22–25.

Telegadas, K. (1971). The seasonal stratospheric distribution and inventories of excess Carbon-14 from March 1955 to July 1969. Health and Safety Laboratories (HASL) Report 243 3-86.

Wilcox, R. W. and Belmont, A. D. (1977). Ozone concentration by latitude, altitude, and month, near 80° W, Rept. No. FAA-AEQ-77-13, U.S. Dept. of Transportation, Washington, D.C., 41 pp.

Young, J. A. and Fairhall, A. W. (1968). Radiocarbon from nuclear weapons tests. *J. geophys. Res. 73*, 1185–1200.

Zimmerman, P. R., Chatfield, R. B., Fishman, J., Crutzen, P. J., Hanst, P. L. (1978). Estimates on the production of CO and H_2 from the oxidation of hydrocarbon emissions from vegetation. *Geophys. Res. Lett. 5*, 679–682.

ЭКСПЕРИМЕНТАЛЬНОЕ СВИДЕТЕЛЬСТВО О ЗНАЧИТЕЛЬНЫХ ЛОКАЛЬНЫХ ФОТОХИМИЧЕСКИХ ИСТОЧНИКАХ ТРОПОСФЕРНОГО ОЗОНА

Обсуждаются широтные и сезонные изменения озона в тропосфере. Особый интерес вызывает неодинаковое поведение этого газа в двух полусферах. Эта асимметрия, в сочетании с диагностичнской фотохимической моделью тропосферы, свидетельствует в пользу той точки зрения, что озон не может рассматриваться, как инертный трассер стратосферного происхождения. Вдобавок, сезонные изменения излишков $^{14}CO_2$ (стратосферный трассер) изучены и сравнены с сезонным изменением озона в течении того же периода наблюдений в том же месте и на той же высоте. Различимые максимумы для озона, которые можно обнаружить в течении лета в нижней тропосфере, не нмеют места для данных по $^{14}CO_2$. Это также предполагает, что фотохимические процессы, имеющие место в тропосфере, являются важным определяющим источником для тропосферного озона.